Role of Hydrogen-Bonded Adducts in Excited-State Proton-Transfer Processes

J. Carlos Penedo, Manuel Mosquera,* and Flor Rodríguez-Prieto*

Departamento de Química Física, Facultade de Química, Universidade de Santiago de Compostela, E-15706 Santiago de Compostela, Spain

Received: April 18, 2000; In Final Form: May 31, 2000

The protonated cation of 2-(2′-hydroxyphenyl)benzimidazole becomes a very strong acid in its first excited singlet state (**C***). We studied the proton-transfer process from **C*** to the bases water, methylurea (MU), and dimethyl sulfoxide (DMSO) in acetonitrile solution by means of fluorescence and UV−vis absorption spectroscopy. We found that the process occurs via a 1:1 hydrogen-bonded adduct between the photoacid **C*** and the base. We determined the photophysical properties of the adducts with the three bases and the equilibrium constants of formation of various adducts in the ground and excited states. The proton transfer takes place by dissociation of the adduct, in a unimolecular or bimolecular process involving a second molecule of the base. The unimolecular dissociation takes place for the adducts formed with DMSO and MU, but not for the adduct formed with water. The bimolecular dissociation occurs for the adducts formed with water and MU. In this process, the entity that finally accepts the proton is a cluster of two molecules of the base. We conclude that only one molecule of water is not able to accept the proton donated by the photoacid, a cluster of two molecules of water being required. This cluster is formed in two consecutive steps. First the adduct between the photoacid and one molecule of water is formed, subsequently followed by the reaction of the adduct with a second molecule of water.

Introduction

Proton-transfer processes are elementary reactions of fundamental importance in chemistry and biology.[1−4] Although a lot of experimental and theoretical research work has been done on this subject, still there is no complete understanding of the molecular mechanisms of these reactions.[5−10] One important area of the current research on the dynamics of proton-transfer processes in solution is concerned with the study of the dissociation of photon-initiated acids (photoacids).[11−17]

It is a well-known fact that the properties of the molecules experience a change in the excited electronic states with respect to the ground state due to the changes in charge density distribution after excitation. When a molecule undergoes an enhancement of acidity in the excited state, the molecule is called a photoacid.[11−17] The excitation of such a molecule generates an acid in an extremely short time. Photoacids have therefore many chemical and technological applications,[18] for example as microenvironment probes for heterogeneous media,[19,20] as initiators in polymerization and depolymerization processes in solid state and in solution,[21] and as a means of inducing a transient pH change ("pH jump").[18] A fundamental utility of photoacids concerns the study of the dynamics of very fast proton-dissociation processes, which take place after the electronic excitation of the photoacid. The process can conveniently be studied by means of fluorescence techniques if the photoacid or its conjugate base are fluorescent or by transient absorption techniques.[17]

Photoacids have been used in the investigation of the dynamics and mechanism of proton transfer to water. Robinson, Lee and collaborators studied the proton-transfer reactions of various neutral weak photoacids (2-naphthol, 1-naphthol, and 1-naphthol-2-sulfonate) in binary mixtures of solvents (alcohol/water and acetonitrile/water) and in aqueous solutions of different salts.[22−30] The rate of the proton transfer was found to have a nonlinear dependence on the water concentration. Using the statistical analysis based on the Markov random walk method, Robinson et al. proposed for these weak photoacids a cluster of 4 ± 1 molecules of water as the proton acceptor.

Agmon, Huppert, Pines and collaborators questioned the interpretation that the dissociation occurs with the involvement of a cluster of water.[31−42] These authors found that the dissociation of 8-hydroxypyrene-1,3,6-trisulfonate (HPTS) occurs in a reversible way, the geminate recombination of the dissociation products taking place in reasonable proportion. Although in this case the recombination is favored by the strong electrostatic interaction between the proton and the quadruple charged anion, these authors showed that this recombination also occurs, although to a minor extent, in other cases, e.g. for 2-naphthol and 1-naphthol, where the anion is only singly charged. Furthermore, investigating the dissociation process of HPTS in an extensive series of methanol/water compositions,[39] they found that the changes of the dissociation rate constant due to the solvent are very close to the variations of the equilibrium constants. They attribute these variations to the localized counterion stability in water-rich solutions, and to proton stability in methanol-rich solutions, challenging the idea that a cluster of water molecules is the required proton acceptor.

The investigations of Tolbert et al. on the proton transfer from different types of derivatives of 1- and 2-naphthol yielded interesting results.[17,43−45] The introduction of alkyl chains containing a varying number of hydroxyl groups on 2-naphthol led to the conclusion that the side chains facilitate the formation of the requisite geometry for proton transfer, affecting the number of water molecules involved.[44] The introduction of electron-withdrawing groups (cyano or methanesulfonyl) resulted in derivatives of very strong acidity in the excited state, comparable in some cases to strong mineral acids.[17,43,45] The photoinduced proton transfer from these acids revealed that the

10.1021/jp001473v CCC: $19.00
Published on Web 07/25/2000

apparent size of the water cluster is a function of the acidity of the proton donor. For strong photoacids, water dimers can be effective proton acceptors. Than Htun et al. came to a similar conclusion after studying the dissociation of the strong photoacid 4-hydroxy-1-naphthalenesulfonate in alcohol/water mixtures.[46−48] In the investigation of the proton transfer to solvent from the cyano naphthols in nonaqueous solvents and water, Agmon et al. and Tolbert et al. found the existence of reversible proton geminate recombination processes and proton-transfer rates controlled by the solvent motion in many instances.[45,49−51]

Pines and Fleming studied the dissociation of protonated 1-aminopyrene in mixtures of solvents.[52] They found that the proton-transfer rate is determined by the proton free energy of transfer from pure water to the binary mixtures, without finding any indication that this rate is determined by the kinetic availability of large water clusters.

Scandola et al. investigated the dissociation of excited protonated *cis*-dicyanobis(2,2′-bipyridine)ruthenium(II) in acetonitrile/water solvent mixtures.[53] They found that the proton has an average hydration number of 3, which could be related to the size of the water clusters acting as proton carriers.

Cations such as 2-(2′-hydroxyphenyl)benzimidazolium,[54] 2-(3′-hydroxy-2′-pyridyl)benzimidazolium,[55] and several hydroxyflavylium[56,57] and hydroxyquinolinium[58−60] ions exhibit a very strong photoacidity, dissociating at the hydroxyl group. Bardez et al. found that the proton ejection rate constant of 7-hydroxyquinolinium cation in concentrated $HClO_4$ solutions depends on the fourth power of the water activity,[59,60] whereas for 6-hydroxyquinolinium cation it depends on the activity of water to the power 2.75.[58]

The aforementioned papers highlight the difficulty of a complete understanding of the molecular details of proton dissociation processes, and especially of proton transfer to water. The purpose of this paper is to illuminate some of the issues involved in this topic. A fundamental question concerns the involvement of water clusters in the proton-transfer process. We studied the dissociation of a strong photoacid in a solvent (acetonitrile) unable to accept the proton. The dissociation takes place only when a base is added. We used water and other nonhydroxylic bases to affect the dissociation. The other bases do not have the ability of water to form dimers, trimers, or higher aggregates through hydrogen bonds. The comparison of the behaviors of the various bases will therefore throw light on the issue of water clusters.

We chose for this study a very strong photoacid, which allowed us to use a low concentration of the base, so that the properties of the solvent hardly altered when that concentration was changed. This should remove the difficulties encountered with weak photoacids, which need a very high concentration of the base for the dissociation rate to compare with the deactivation rate of the photoacid, and therefore the solvent properties and associated magnitudes also change with the concentration of the base.

Unlike most of the photoacids used in previous investigations of the dissociation process, which are neutral (naphthol and derivatives) or negatively charged (HPTS), the photoacid that we will discuss here is a cation. This causes a lesser tendency of the dissociation products to recombine, since the dissociation in the aforementioned cases generates a pair of ions (the negatively charged conjugate base and the proton), while in our case the conjugate base is a neutral species. This should simplify the kinetics of the proton transfer.

The photoacid we used is the protonated form of 2-(2′-hydroxyphenyl)benzimidazole (HBI), which we will call hereinafter cation **C*** (Scheme 1). We showed in a previous article that this excited cation acts as a very strong photoacid, which dissociates completely in aqueous solutions ($pK_a^* \approx -3$, Förster cycle) and in considerable proportion in ethanol.[54] The excited cation **C*** dissociates at its hydroxyl group, leaving an excited neutral molecule, whose electronic structure is usually represented by its resonance keto form (**K***, Scheme 1), although also a resonance zwitterionic form may be drawn with the negative charge on the oxygen and the positive charge on the benzimidazole N. Since both the photoacid **C*** and its conjugate base **K*** show fluorescence, it is possible to investigate the photodissociation process by means of this technique. In solvents that are unable to accept the proton, e.g. acetonitrile, the dissociation does not occur, unless water or other bases are added. In this article we will discuss the results of our study on the photodissociation of the cation **C*** in acetonitrile in the presence of low concentrations of water and two other bases: dimethyl sulfoxide (DMSO) and methylurea (MU). Although the basicity of these species is low (pK_a of its conjugate acid: −1.7 (H_2O), −1.5 (DMSO),[61] and 0.9 (MU)),[62] it is sufficient in this case because of the strong acidity of the excited cation **C***. Stronger bases may not be used, because they will be protonated in the acidic medium that is necessary to protonate HBI in order to get the cation **C**. We found that hydrogen-bonded adducts between the photoacid and the base play a central role in the proton-transfer process, a feature not described in previous studies of other photoacids.

SCHEME 1: Proton Transfer from the Excited Cation of 2-(2′-hydroxyphenyl)benzimidazole to a Base B

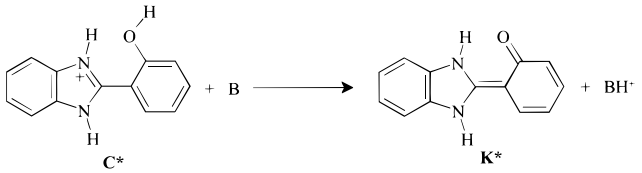

Experimental Section

HBI and the methoxy derivative 2-(2′-methoxyphenyl)-benzimidazole (MBI) were obtained, purified, and characterized as described in a previous paper.[54] Solutions were made up in spectroscopy grade acetonitrile (Scharlau). Spectroscopy grade dimethyl sulfoxide (Scharlau), *N*-methylurea (Aldrich, 99%), and double distilled water were employed. All experiments were carried out at 25 °C, and none of the solutions were degassed. To obtain an acidic medium in acetonitrile, $HClO_4$ (Merck p.a.) in the concentration range $10^{-4}-10^{-3}$ mol dm^{-3} was used. We checked by UV−vis absorption spectroscopy and fluorescence excitation that the monocation is the only species present in the ground state under these conditions and that this acidic medium is maintained after the addition of the base. The concentration of residual water in acetonitrile, determined by the Karl Fischer method, was 5×10^{-3} mol dm^{-3}. This value, together with the water accompanying perchloric acid, $[H_2O] = 2.4\ [HClO_4]$, makes a maximum concentration of water in the solutions before addition of the base of 1.9×10^{-2} mol dm^{-3}. Fluorescence quantum yields were determined using quinine sulfate in aqueous H_2SO_4 as standard ($\phi = 0.546$).[54] To determine the equilibrium constants of formation of the adducts between the cation **C** and the bases MU or DMSO, we measured the absorption of a solution of **C** at various concentrations of the base, obtained by adding microliter amounts of MU or DMSO to a 3 mL solution of **C**.

UV−vis absorption spectra were recorded on a Cary 3E Varian spectrophotometer. Fluorescence excitation and emission

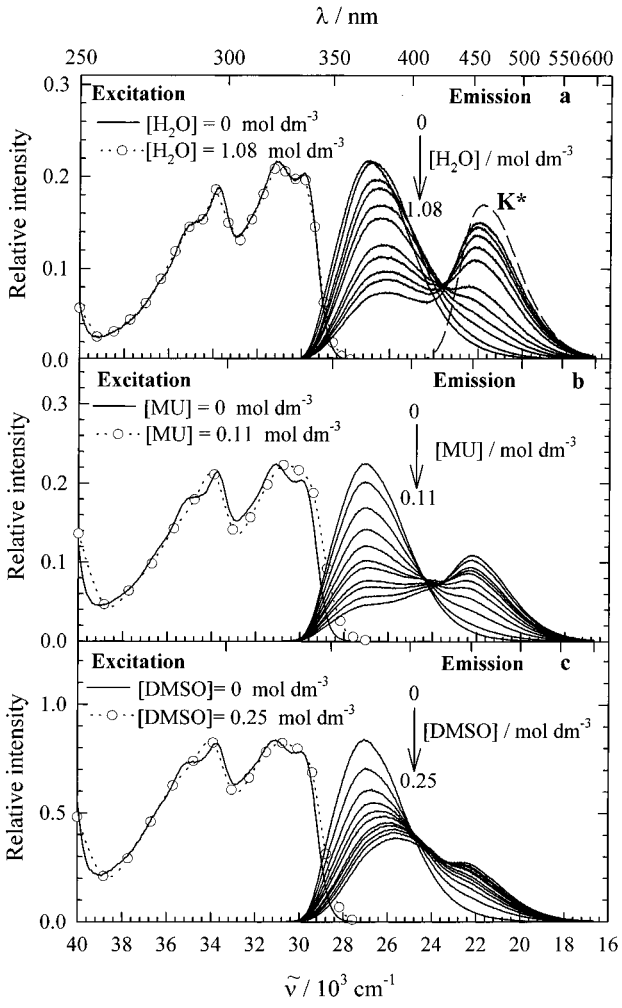

Figure 1. Fluorescence excitation and emission spectra of HBI in acidified acetonitrile solution with increasing concentrations of (a) water ($[HClO_4] = 6.0 \times 10^{-4}$ mol dm^{-3}), (b) methylurea ($[HClO_4] = 5.1 \times 10^{-3}$ mol dm^{-3}), and (c) dimethyl sulfoxide ($[HClO_4] = 2.5 \times 10^{-3}$ mol dm^{-3}): (—) $\tilde{\nu}_{em} = 26\,700$ cm^{-1}; (- - ○ - -) $\tilde{\nu}_{em} = 22\,200$ cm^{-1}; $\tilde{\nu}_{exc} = 31\,700$ cm^{-1}. [HBI] $= 9 \times 10^{-6}$ mol dm^{-3}. For comparison, the fluorescence emission spectrum of HBI in neutral acetonitrile in the absence of water, corresponding to the keto form **K***, is also shown in the upper panel (— —).

spectra were recorded on a Spex Fluorolog-2 FL340 E1 T1 spectrofluorometer, with correction for instrumental factors by means of a rhodamine B quantum counter and correction files supplied by the manufacturer. Fluorescence lifetimes were determined by time-correlated single-photon counting on an Edinburgh Instruments CD-900 spectrometer equipped with a hydrogen-filled nanosecond flash lamp and the analysis software supplied by the manufacturer. The instrumental response width of the system is 1.0 ns. We measured usually until 10 000 counts were reached in maximum (2×10^3 channels, 24 ps/channel). The emission band-pass for the lifetime measurements was usually 20 nm.

Results

(1) Proton Transfer from Photoacid C* to Water. The fluorescence spectrum of HBI in acidified acetonitrile showed a single emission band ($\tilde{\nu}_{max} = 27\,000$ cm^{-1}; fluorescence quantum yield, $\phi_C = 0.32$) with a normal Stokes shift (Figure 1). This emission resembles that obtained for HBI in other acidified solvents and can be attributed to the cation **C***,[54] so we will call it hereafter band C. Upon addition of small amounts

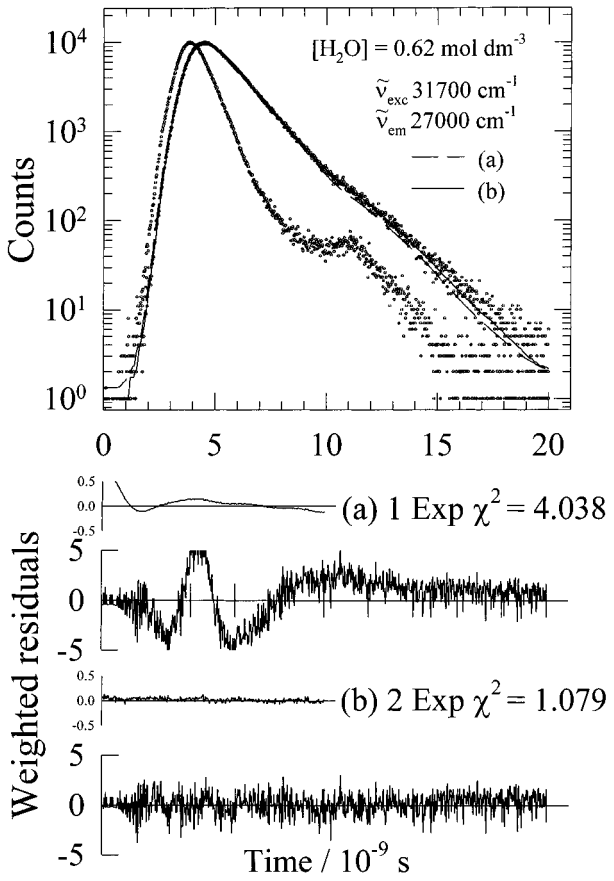

Figure 2. Band C fluorescence decay of HBI in acidified acetonitrile solution ($[HClO_4] = 7.9 \times 10^{-4}$ mol dm^{-3}) with $[H_2O] = 0.62$ mol dm^{-3}, lamp profile, and the results of (a) monoexponential ($\tau = 1.22 \pm 0.01$ ns) and (b) biexponential ($\tau_1 = 1.429 \pm 0.006$ ns, $\tau_2 = 0.37 \pm 0.01$ ns) fits. The weighted residuals and autocorrelation functions are also shown. [HBI] $= 1.1 \times 10^{-5}$ mol dm^{-3}.

of water, the fluorescence band C was quenched and a new red-shifted emission band appeared with its maximum at 22 000 cm^{-1} (Figure 1a), which is very similar to that of the neutral keto form **K*** in water, in ethanol, or in other solvents.[54,63−65] This emission band will be called hereafter band K. For comparison, we show in Figure 1a the fluorescence spectrum of HBI in neutral acetonitrile in the absence of water. This spectrum corresponds to the keto form **K***, which is formed in these conditions from the enol form existing in the ground state by excited-state intramolecular proton transfer.[54,63−65] The fluorescence quantum yield of the **K*** emission in neutral acetonitrile was 0.25.

These results mean that the addition of water to an acidified acetonitrile solution of HBI gives rise to the photodissociation of **C*** according to Scheme 1. The excitation spectrum was independent of the water concentration and of the monitoring emission wavenumber (Figure 1a) and coincided with the absorption spectrum. Note that no isoemissive point was observed upon varying the water concentration within the range 0−1 mol dm^{-3}. The fluorescence emission spectra were independent of the excitation wavenumber.

The fluorescence of the protonated methoxy derivative MBI in acidified acetonitrile solutions was unaffected by varying the water concentration, showing only the band C. This supports our interpretation that the protonated HBI photodissociates at the hydroxyl upon adding water.

The fluorescence decay of HBI in acidified acetonitrile was measured at several monitoring wavenumbers and with various

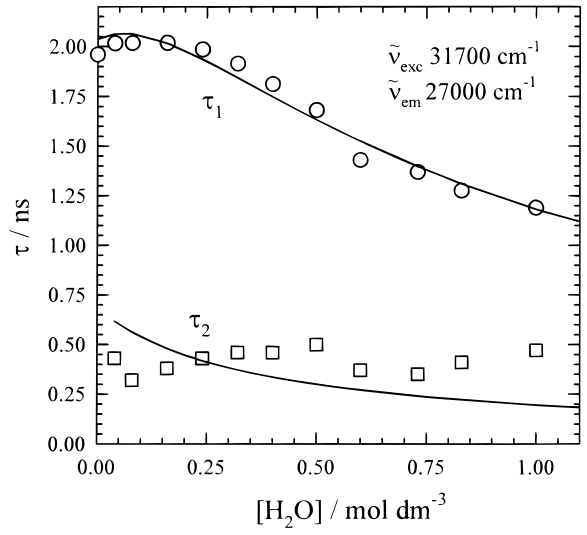

Figure 3. Decay times of the biexponential decays of band C fluorescence obtained for HBI in acidified acetonitrile solution ([$HClO_4$] $= 7.9 \times 10^{-4}$ mol dm^{-3}) with increasing water concentrations. The solid lines are the result of the global fit of the equations deduced from the proposed mechanism in Scheme 4 to represent the dependence of the fluorescence intensities and decay times on water concentration. [HBI] $= 1.1 \times 10^{-5}$ mol dm^{-3}.

water concentrations. In the absence of water, the decay of the single emission band (band C) was monoexponential, with a lifetime of 1.91 ± 0.02 ns. Upon addition of water, the decay of this band became biexponential (Figure 2). Figure 3 shows the values of the two decay times obtained at various water concentrations. One of the components had a decay time (τ_1) which increased slightly with the water concentration at low concentrations, followed by a decrease at higher concentrations The contribution to the decay of this exponential component fell with increasing water concentration, whereas that of the second exponential component rose. For the second component, a decay time (τ_2) around 0.4 ns was obtained, which does not vary significantly with the water concentration.

The fluorescence decay of band K, which appeared in the presence of water, was triexponential (Figure 4). The decay times of two of the components were (within the experimental error) similar to those obtained by measuring the decay of band C. The third component had a constant decay time (3.7 ± 0.1 ns) at the different water concentrations.

(2) Proton Transfer from Photoacid C* to Dimethyl Sulfoxide. Addition of DMSO to an acidified acetonitrile solution of HBI resulted in a slight change in the absorption spectrum (Figure 5). This change was not observed when water was added. The fluorescence band C was quenched by the addition of DMSO, accompanied by a red shift of its maximum (Figure 1c). The quenching of band C was concomitant with the appearance of band K. Both the fluorescence excitation and absorption spectra showed the same slight changes upon adding DMSO. Furthermore, the fluorescence excitation and emission spectra depended on the monitoring wavenumber. None of the above-mentioned spectral changes due to the addition of DMSO was observed for the methoxy derivative MBI.

The fluorescence decay of HBI in acidified acetonitrile in the presence of DMSO exhibited features similar to those observed in the presence of water. Band C showed a biexponential decay (Figure 6). One of the components showed decreasing decay time (τ_1) and contribution to the decay upon increasing the DMSO concentration. The second component had a decay time (τ_2, around 2.1 ns) which did not change

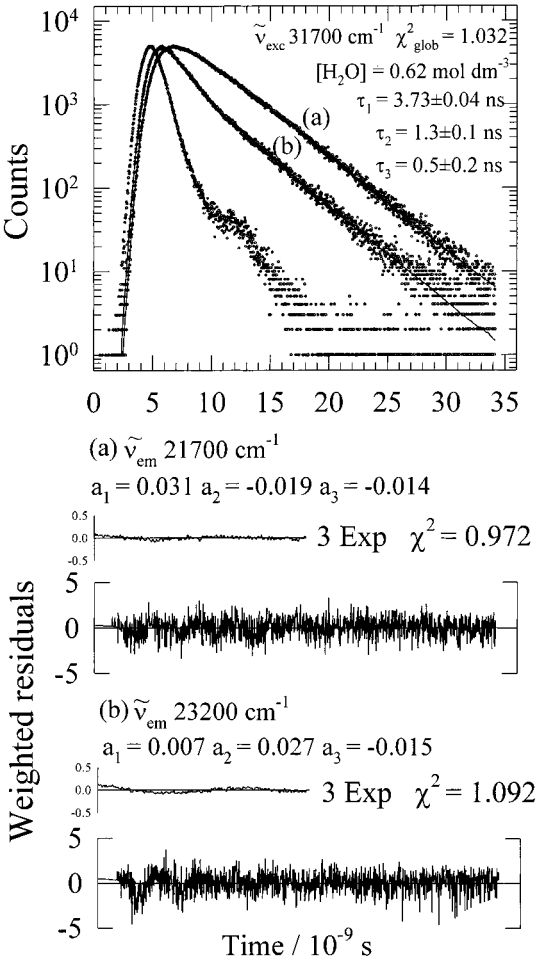

Figure 4. Fluorescence decay of HBI in acidified acetonitrile solution ([$HClO_4$] $= 7.9 \times 10^{-4}$ mol dm^{-3}) with [H_2O] = 0.62 mol dm^{-3} at (a) $\tilde{\nu}_{em} = 21\,700$ cm^{-1} and (b) $\tilde{\nu}_{em} = 23\,200$ cm^{-1} and lamp profile ($\tilde{\nu}_{exc} = 31\,700$ cm^{-1}). The figure shows also the results of the global analysis of the decay data collected at both emission wavenumbers to fit a triexponential decay function. The fluorescence decay times τ_i, associated amplitudes a_i, weighted residuals, and autocorrelation functions are shown. [HBI] $= 1.1 \times 10^{-5}$ mol dm^{-3}.

significantly by varying the DMSO concentration, while its contribution to the decay rose with increasing DMSO concentration and also when the decay was monitored at lower wavenumbers. The decay of band K was triexponential, and two of its components coincided (within the experimental error) with those obtained by monitoring the fluorescence decay in band C, while the third component had a constant decay time of 3.9 ± 0.1 ns.

(3) Proton Transfer from Photoacid C* to Methylurea. The UV−vis absorption spectrum of HBI in acidified acetonitrile changed slightly upon adding MU. The fluorescence excitation spectrum showed similar changes (Figure 1b).

The fluorescence emission spectrum of HBI changed also in the presence of MU (Figure 1b). The fluorescence intensity of band C fell and that of band K rose as the MU concentration increased. The most striking difference with respect to the experiments carried out with the bases water and DMSO was the appearance of a shoulder around 24 000 cm^{-1} in the fluorescence spectra. Moreover, the fluorescence excitation and emission spectra depended on the monitoring wavenumber (Figure 5). None of the above-mentioned spectral changes due to the addition of MU was observed for the methoxy derivative MBI.

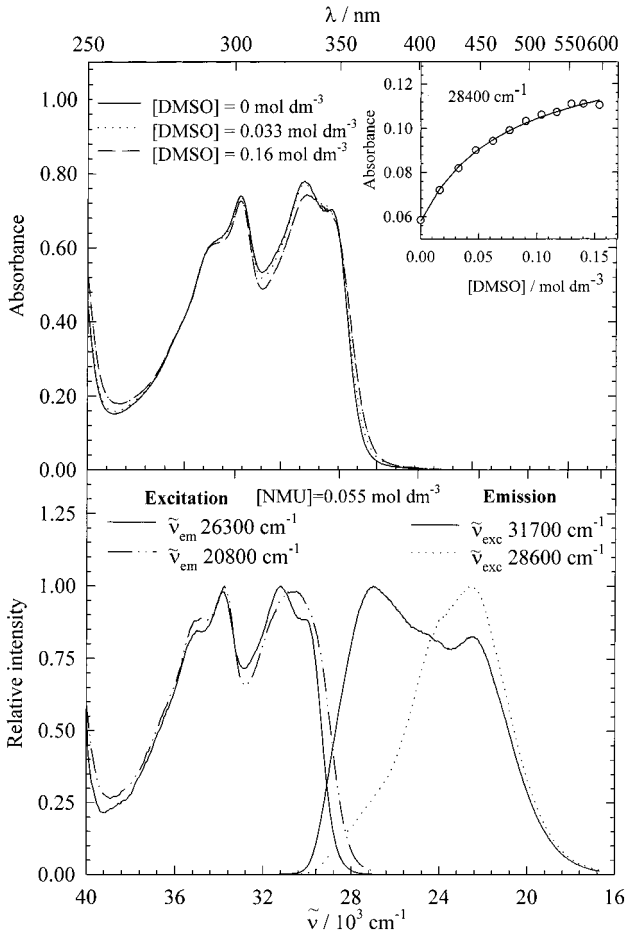

Figure 5. (Top) Absorption spectra of HBI ([HBI] = 3.3×10^{-5} mol dm^{-3}) in acidified acetonitrile solution ([$HClO_4$] = 2.7×10^{-3} mol dm^{-3}) with increasing concentration of dimethyl sulfoxide. The insert shows the [DMSO] dependence of the absorbance at 28 400 cm^{-1}. (Bottom) Monitoring-wavenumber dependence of the fluorescence excitation and emission spectra of HBI ([HBI] = 9.3×10^{-6} mol dm^{-3}) in acidified acetonitrile solution ([$HClO_4$] = 5.6×10^{-3} mol dm^{-3}) with [MU] = 0.055 mol dm^{-3}.

When being monitored at band C (28 600 cm^{-1}), the fluorescence decay was monoexponential, with decreasing lifetime (τ_C) as the concentration of MU increased. The reciprocal of τ_C showed a linear dependence on MU concentration (Figure 7). When being monitored at 24 000 cm^{-1}, the fluorescence decay at any MU concentration could also be described by a monoexponential function, although its decay time was larger than that obtained at 28 600 cm^{-1} at the same MU concentration. Given that the cation **C*** also emitted in considerable proportion at 24 000 cm^{-1} (Figure 1), it is reasonable to assume that the decay time τ_C (measured at 28 600 cm^{-1}) contributes to the decay at 24 000 cm^{-1}. We therefore fitted a biexponential function to the fluorescence decay data collected at 24 000 cm^{-1}, keeping one of the decay times constant at the value of τ_C measured at 28 600 cm^{-1} at the same MU concentration. The obtained fits showed a better residuals distribution and a lower χ^2 value, the second decay time (denoted as τ_A) only being slightly larger than the first one (τ_C). It seems reasonable to assume that this fact causes the impossibility of the fit process to separate both components. The reciprocal of τ_A also showed a linear dependence on [MU] (Figure 7). The contribution of the exponential term τ_C fell and the contribution of τ_A rose as the MU concentration increased.

The fluorescence decay at 20 000 cm^{-1} could be described by a biexponential function, one of the components showing

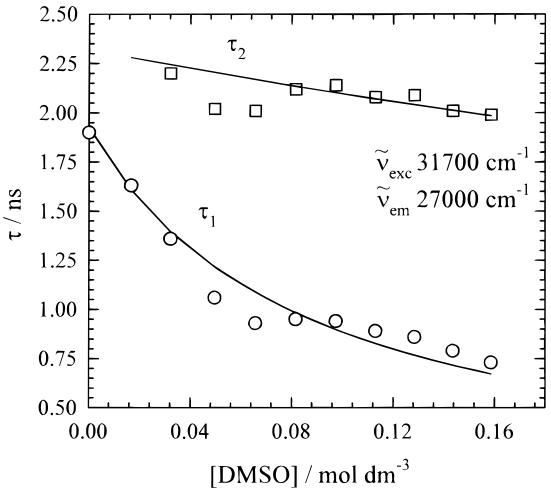

Figure 6. Decay times of the biexponential decays of band C fluorescence obtained for HBI in acidified acetonitrile solution ([$HClO_4$] = 2.7×10^{-3} mol dm^{-3}) at different dimethyl sulfoxide concentrations. The solid lines are the result of the global fit of the equations deduced from the proposed mechanism in Scheme 3 to represent the dependence of the fluorescence intensities and decay times on DMSO concentration. [HBI] = 2.6×10^{-5} mol dm^{-3}.

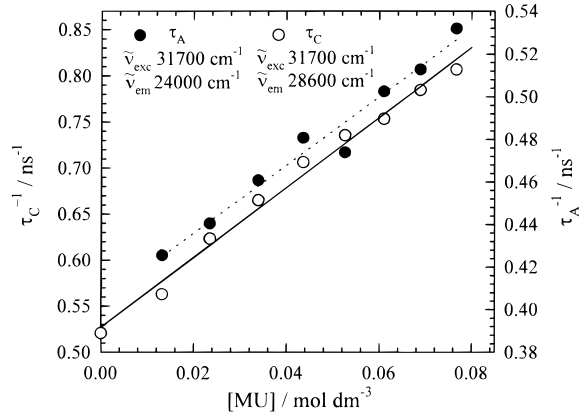

Figure 7. Dependence of the reciprocals of the fluorescence decay times of HBI in acidified acetonitrile solution ([$HClO_4$] = 5.7×10^{-3} mol dm^{-3}) on the concentration of methylurea and linear correlation. (○) Decay times (τ_C) of the monoexponential decays of band C fluorescence. (●) τ_A component of the biexponential decay at 24 000 cm^{-1} (the decay time of the second exponential component was fixed at the value of τ_C obtained from the monoexponential decay of band C). [HBI] = 1.0×10^{-5} mol dm^{-3}.

negative amplitude. The rise time showed an intermediate value between the two decay times measured at 24 000 cm^{-1}. When a triexponential function was fitted to the fluorescence data, with two decay times fixed at the values obtained at 24 000 cm^{-1}, the fits became better and a third lifetime was obtained with a constant value of 3.61 ± 0.05 ns and a positive amplitude, whereas the other components had negative amplitudes.

Discussion

(1) Proton Transfer from C* to Methylurea. Both the absorption and the fluorescence excitation spectrum of HBI in acidified acetonitrile (corresponding to the cation **C**) changed due to the presence of methylurea (Figure 1b), while these spectral changes were not observed for the methoxy derivative MBI. This behavior suggests that in the ground state an interaction exists between the cation **C** and MU via the hydroxyl

SCHEME 2: Mechanism of the Proton Transfer from the Cationic Photoacid C* to the Base Methylurea (MU) in Acetonitrile Solution

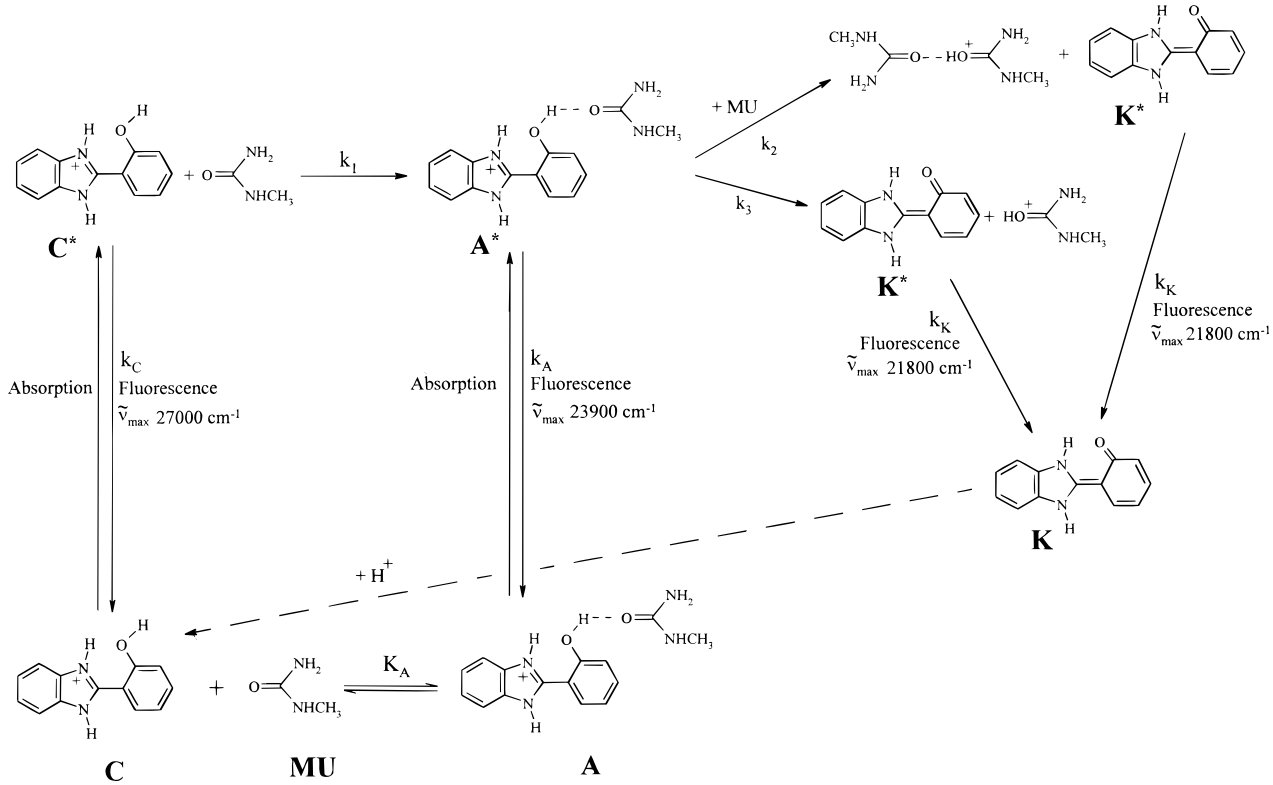

group (−O−H···O═C<), which may result in the formation of a hydrogen-bonded adduct. Similar adducts are well-known, such as for example the adducts between phenol and amides[66] or the adducts between hydroxyaromatic compounds and various proton acceptors.[13,67−71] The formation of a hydrogen bond donated from the hydroxylic hydrogen atom to the solvent was also clearly demonstrated on studying the solvatochromism of the photoacids β-naphthol and 5-cyano-2-naphthol.[72−74]

The observed change of the absorption at different concentrations of MU may be explained by the formation of a hydrogen-bonded adduct (called **A** in Scheme 2) between the cation **C** and MU. Since the concentration of **C** is much lower than that of MU, it seems reasonable to consider the MU concentration unaffected by the formation of the adduct, and the absorbance at a given wavenumber (A_ν) will therefore depend on the MU concentration as described by eq 1, in which K_A is the equilibrium constant of formation of the adduct (expressed as the quotient of concentrations, $K_A = [A]/[C][MU]$), and a_ν and b_ν are parameters which are dependent on the concentration of **C** before formation of the adduct, $[\mathbf{C}]_0$, and on the molar absorption coefficients of the adduct (ε_A) and the cation (ε_C) at the given wavenumber: $a_\nu = \varepsilon_C[\mathbf{C}]_0$, $b_\nu = \varepsilon_A K_A[\mathbf{C}]_0$.

$$A_\nu = \frac{a_\nu + b_\nu[\mathrm{MU}]}{1 + K_A[\mathrm{MU}]} \qquad (1)$$

The fit of eq 1 to the absorption data is good (see in Figure 5 the result of a similar fit with the data set obtained for DMSO), yielding a value of $K_A = 12.7 \pm 0.1$ dm^3 mol^{-1}, in the same order of magnitude found for similar adducts of hydroxyaromatic compounds.[13,66−68] Within the experimental error, the same value of K_A was found at various detection wavenumbers.

Figure 1b displays the influence of MU on the fluorescence spectrum of HBI in acidified acetonitrile. In the absence of MU, the spectrum (band C) stems from the cation **C***, which has a lifetime of 1.91 ± 0.02 ns. In the presence of MU, band K appears due to the formation of the keto species **K*** by dissociation of the cation **C***, and, as a result of this, the intensity of band C decreases. The emission spectrum, however, shows a shoulder around 24 000 cm^{-1}, between the C and K bands, which cannot be associated with the emissions from the species **C*** and **K***, indicating the presence of a third emitting species, which might be the excited adduct **A***. The fluorescence spectra of the hydrogen-bonded adducts of hydroxyaromatic compounds are well-known.[13,67,69,71]

The emission spectrum of **A*** was obtained by two different procedures. In the first procedure, we assumed that the contribution of **A*** to the emission spectrum of HBI in the presence of MU was negligible at high ($\tilde{\nu}$ > 28 000 cm^{-1}) and low ($\tilde{\nu}$ < 19 000 cm^{-1}) wavenumbers. In these spectral regions the spectra of **C*** and **K*** (obtained in the absence of MU in acidic medium and in neutral medium, respectively) were normalized with the spectrum obtained in the presence of MU, and subsequently subtracted from this spectrum to yield the spectrum of **A***. This procedure yields a well-shaped band for **A*** (see Figure 8), which confirms the contribution of the adduct to the spectra.

The emission spectrum of **A*** was also obtained by applying the method of principal components analysis (PCA)[75−79] to the series of spectra of HBI in acidified acetonitrile in the presence of various concentrations of MU.[80] This method gives information (through the eigenvectors of a square matrix constructed from the fluorescence spectra recorded at different MU concentrations) about the minimal number of spectral components necessary to reproduce the experimental spectra. In this case, the obtained number of independent components was three. Using the physical meaningful restrictions that the spectral components should have a positive intensity and that each experimental spectrum should be a linear combination of the

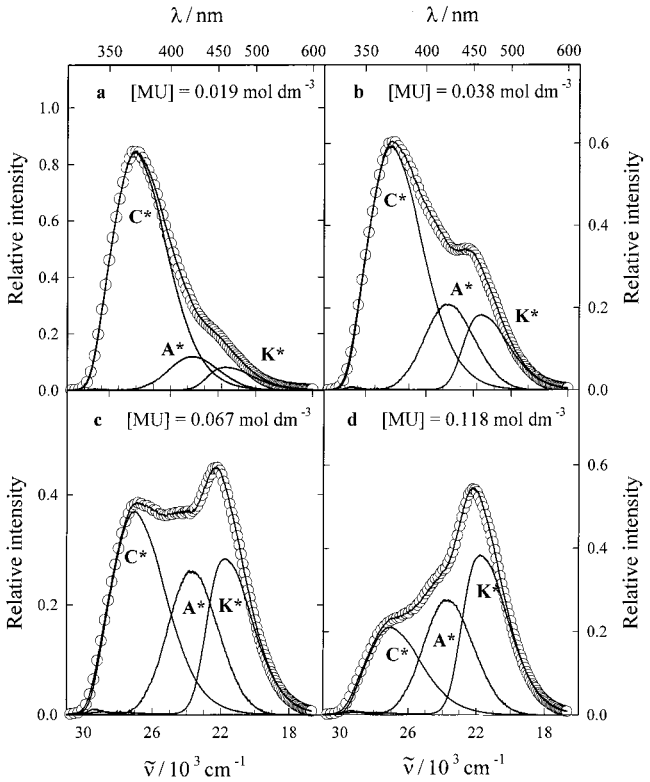

Figure 8. Experimental (—) fluorescence spectra of HBI in acidified acetonitrile solution ($[HClO_4] = 5.1 \times 10^{-3}$ mol dm^{-3}) with various methylurea concentrations and calculated spectra (— ○ —) obtained by fitting a linear combination of the fluorescence spectra of **C***, **A***, and **K***. The individual contributions of these spectra are also shown. $\tilde{\nu}_{exc} = 31\,700$ cm^{-1}. $[HBI] = 9.3 \times 10^{-6}$ mol dm^{-3}.

three independent components with positive contribution coefficients, we obtained the three spectral components given in Figure 8. The spectra assigned to **C*** and **K*** match well with the experimentally obtained ones, while the spectrum assigned to **A*** is in excellent agreement with the one obtained by the normalization method.

Figure 8 depicts the decomposition of various experimental emission spectra of HBI in the presence of different concentrations of MU as a linear combination of the three independent components. As can be observed, the experimental spectra are in very good agreement with the linear combinations.

The decomposition of the spectrum of HBI at different concentrations of MU yields the contribution coefficients of the individual fluorescence spectra of **C***, **K***, and **A*** to each experimental spectrum (emission coefficients F_C, F_K, and F_A representing the relative intensity of each species). In Figure 9 we show the values obtained for these coefficients, relative to the value of the emission coefficient of the cation **C*** in the absence of MU, F_C^0. As can be seen, nonlinear correlations between the coefficients and the concentration of MU are observed. The insert in Figure 9 shows the ratio of the emission coefficients of the cation (F_C^0/F_C) plotted against the concentration of MU. The observed nonlinear dependence implies that the quenching of the cation does not follow the Stern−Volmer relation, as expected due to the formation in the ground state of the adduct **A** between the cation **C** and MU.

In Figure 9, the ratios of the emission coefficients of the fluorescent species are plotted against the concentration of MU. Almost linear correlation with [MU] is observed for the ratios of the emission coefficients of **A*** and **C*** (F_A/F_C) and of **K*** and **A*** (F_K/F_A), implying that the transformations of **C*** into **A*** and of **A*** into **K*** are induced by MU. Thus, **A*** acts as an

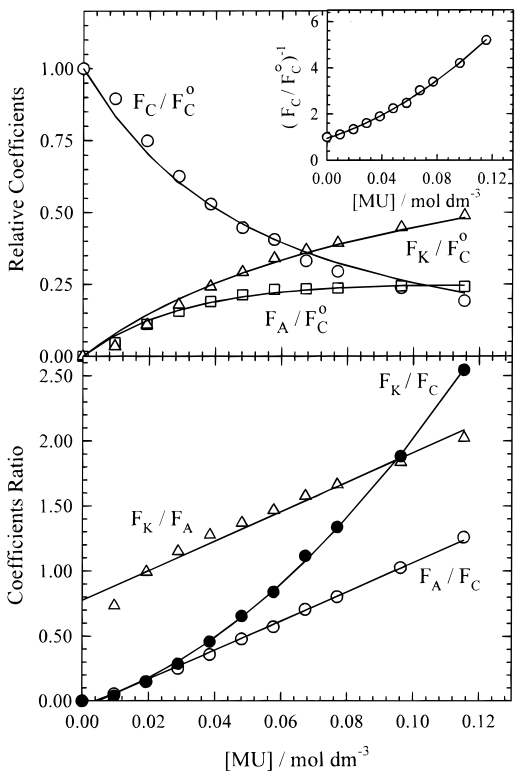

Figure 9. (Top) Emission coefficients expressing the relative contributions of the individual fluorescence spectra of **C***, **A***, and **K*** to the fluorescence spectra of HBI in acidified acetonitrile solution ($[HClO_4] = 5.1 \times 10^{-3}$ mol dm^{-3}) with increasing methylurea concentration. F_C^0 is the emission coefficient of **C*** in the absence of MU. The solid lines are the result of the global fit of eqs 2−6 to the emission coefficients and decay time data. The insert shows the [MU] dependence of the reciprocal of the relative emission coefficient of **C***. (Bottom) [MU] dependence of the ratios of the emission coefficients. $\tilde{\nu}_{exc} = 31\,700$ cm^{-1}. $[HBI] = 9.3 \times 10^{-6}$ mol dm^{-3}.

intermediate species between **C*** and **K***, MU thereby participating both in its formation and in its disappearance to generate **K***. Note that the ratio of the emission coefficients of **K*** and **A*** (F_K/F_A) is linear with the MU concentration, with an intercept different from zero, indicating that the adduct is able to dissociate to generate **K*** without the involvement of a second molecule of MU, although the latter favors this process (Scheme 2).

The contribution of the adduct to the spectra of HBI in acidified acetonitrile in the presence of MU can also be derived from Figure 5, in which the dependence of the excitation and emission spectra on the monitoring wavenumber is shown. Monitoring in the maximum of band C yields the excitation spectrum of **C***, while monitoring in band K gives an excitation spectrum which is slightly different due to the adduct contribution, most significantly in the spectral region around 28 000 cm^{-1}. When exciting in this region, mainly the contributions of **A*** (shoulder at 24 000 cm^{-1}) and **K*** are observed in the emission spectrum.

The fluorescence decay of band C at 28 600 cm^{-1} is monoexponential. The reciprocal of its lifetime (τ_C^{-1}) varies linearly with the concentration of MU (Figure 7). This behavior is in agreement with the above-mentioned quenching process undergone by the excited cation **C*** to yield the adduct **A*** (Scheme 2). The fact that the decay of **C*** is monoexponential indicates that the quenching process is irreversible and that the fluorescence at 28 600 cm^{-1} exclusively stems from **C***, without any contribution from the adduct. This is consistent with the spectral decomposition analysis shown in Figure 8.

TABLE 1: Equilibrium Constants *K*, Rate Constants *k*, and Fluorescence Quantum Yields ϕ Obtained for the Proton Transfer from the Cationic Photoacid C* to the Bases Methylurea (MU), Dimethyl Sulfoxide (DMSO), and Water in Acetonitrile Solution

	MU	DMSO	Water
$K_A/(dm^3\ mol^{-1})$	12.7 ± 0.1	13.3 ± 0.1	
$K_{A^*}/(dm^3\ mol^{-1})$	$>4 \times 10^2$	$(8 \pm 3) \times 10$	3.5 ± 0.5
$k_1/(dm^3\ mol^{-1}\ s^{-1})$	$(3.9 \pm 0.1) \times 10^9$	$(5.4 \pm 0.4) \times 10^9$	$(3.5 \pm 0.4) \times 10^9$
k_{-1}/s^{-1}	$<1 \times 10^7$	$(7 \pm 1) \times 10^7$	$(1.0 \pm 0.1) \times 10^9$
$k_2/(dm^3\ mol^{-1}\ s-1)$	$(1.59 \pm 0.08) \times 10^9$		$(5.5 \pm 0.8) \times 10^8$
k_3/s^{-1}	$(1.3 \pm 0.3) \times 10^8$	$(2 \pm 1) \times 10^8$	
k_A/s^{-1}	$(2.7 \pm 0.3) \times 10^8$	$(3 \pm 2) \times 10^8$	$(4.2 \pm 0.5) \times 10^8$
ϕ_A	0.18	0.48	0.29
ϕ_K/ϕ_C	1.0 ± 0.1	0.9 ± 0.8	1.4 ± 0.2

The fluorescence decay at 24 000 cm^{-1}, where the adduct **A*** has its emission maximum, is biexponential. One of the decay times coincides with that of the cation **C*** (τ_C), as it was expected given the contribution of the emission of **C*** at this wavenumber (see Figure 8). In agreement with our interpretation of the formation and decay of the excited adduct **A*** (Scheme 2), its fluorescence decay would show a rise time τ_C, corresponding to the decay of its precursor **C***. We think therefore that the decay time τ_C measured at 24 000 cm^{-1} corresponds to the decay of **C*** and also to the rise time of **A***. The second decay time measured in these conditions (τ_A) may be attributed to the rate of disappearance of **A***. Since the reciprocal of τ_A shows a linear dependence on the concentration of MU (Figure 7), the disappearance of **A*** would be favored by MU, as was already concluded from the spectral decomposition and the obtained emission coefficients.

The fluorescence decay at 20 000 cm^{-1} is triexponential. Two of the exponential components have negative amplitudes and similar decay times, corresponding to those measured at 24 000 cm^{-1}, whereas the third component shows a positive amplitude and a decay time (3.61 ± 0.05 ns) independent of the MU concentration. The latter decay time coincides with that of the neutral keto species **K*** in acetonitrile (3.7 ns).[63] According to the spectral decomposition shown in Figure 8, the fluorescence emission at 20 000 cm^{-1} should show a major contribution from the emission of **K*** and a minor contribution from **A***. The triexponential decay measured at 20 000 cm^{-1} is therefore consistent with Scheme 2, since the decay of **K*** should be triexponential, two of the decay times coinciding with those of the biexponential decay of **A***. The interpretation of the values of the amplitudes is not easy, since the fluorescence is composed from the emission of **K*** and **A***, which would contribute with a different sign to two of the exponential terms. Moreover, we should note that the amplitudes are the parameters determined with more uncertainty in the fitting procedure.

In view of the above results, we propose that the proton-transfer process from the photoacid to the MU takes place via the two routes depicted in Scheme 2. In one of the routes only one molecule of MU participates, while in the other route two molecules of MU are involved. Both routes proceed via the hydrogen-bonded adduct **A***, formed between MU and the excited cation. This excited adduct can be formed from its components or by excitation of the ground-state adduct **A**. The excited adduct **A*** can dissociate directly, yielding the protonated MU and **K***, or, in a parallel route, react with a second molecule of MU to afford also **K***. The induction of the dissociation of the adduct by MU is probably related to the stabilization of the protonated MU by formation of a hydrogen-bonded dimer with the second molecule of MU (Scheme 2).

From the proposed mechanism in Scheme 2, eqs 2−6 have been deduced (see Supporting Information), which show the dependence of the emission coefficients and decay times on the concentration of MU in which $\alpha = k_C k_{rA}/k_{rC}k_2$, $\beta = k_{rK}k_C/k_K k_{rC}$, $\gamma = k_1/k_C$, $\delta = (k_A + k_3)/k_2$, $\varepsilon = \varepsilon_A/\varepsilon_C$, and $\chi = k_3/k_2$.

$$\frac{F_C}{F_C^0} = \frac{1}{(1+\gamma[MU])(1+K_A[MU])} \quad (2)$$

$$\frac{F_A}{F_C^0} = \frac{\alpha(\varepsilon K_A[MU](1+\gamma[MU]) + \gamma[MU])}{(1+K_A[MU])(\delta+[MU])(1+\gamma[MU])} \quad (3)$$

$$\frac{F_K}{F_C^0} = \frac{\beta(\chi+[MU])\{\varepsilon K_A[MU](1+\gamma[MU]) + \gamma[MU]\}}{(1+K_A[MU])(\delta+[MU])(1+\gamma[MU])} \quad (4)$$

$$\tau_C^{-1} = k_C + k_1[MU] \quad (5)$$

$$\tau_A^{-1} = k_A + k_3 + k_2[MU] \quad (6)$$

In these relations, k_r is the radiative deactivation constant of the corresponding species, and ϵ_A and ϵ_C are the molar absorption coefficients of the adduct and the cation, respectively, at the given wavenumber.

According to these equations, the proposed mechanism predicts linear dependencies of F_K/F_A, τ_C^{-1}, and τ_A^{-1} vs [MU], which were experimentally observed (Figures 7 and 9). Equations 2−6 were globally fitted to the experimental results, affording satisfactory fits (see the solid lines in Figure 9) and yielding the values of the parameters listed in Table 1.

From the values of the fit parameters, we can obtain the following relations of the fluorescence quantum yields ϕ_i, which represent the quantum yield of each species *i* if they could be directly excited and exclusively deactivated by fluorescence, internal conversion, and intersystem crossing (rate constant of radiative decay, k_r; rate constant of total decay, *k*):

$$\frac{\phi_A}{\phi_X} = \frac{k_C k_{rA}}{k_{rC} k_A} = \frac{\alpha k_2}{k_A} \quad (7)$$

$$\frac{\phi_K}{\phi_C} = \frac{k_{rK} k_C}{k_K k_{rC}} = \beta \quad (8)$$

Since the fluorescence quantum yield of the cation **C*** in acetonitrile is known ($\phi_C = 0.32$), we can calculate from the experimental value of the ratio ϕ_A/ϕ_C the quantum yield of the adduct. The value obtained ($\phi_A = 0.18$) is of the same order of magnitude as the quantum yield of the cation **C***.

The value obtained for the ratio of quantum yields $\phi_K/\phi_C = 1.0 \pm 0.1$ means that the quantum yield of **K*** must be very similar to that of **C*** (0.32). The quantum yield of **K*** cannot be determined directly in acetonitrile, because it does not exist in the ground state. When HBI is excited in its neutral form (enol) in acetonitrile, only the fluorescence of **K*** was detected, and a fluorescence quantum yield of 0.25 was measured in these conditions. Since the enol form does not fluoresce, its main

SCHEME 3: Mechanism of the Proton Transfer from the Cationic Photoacid C* to the Base Dimethyl Sulfoxide (DMSO) in Acetonitrile Solution

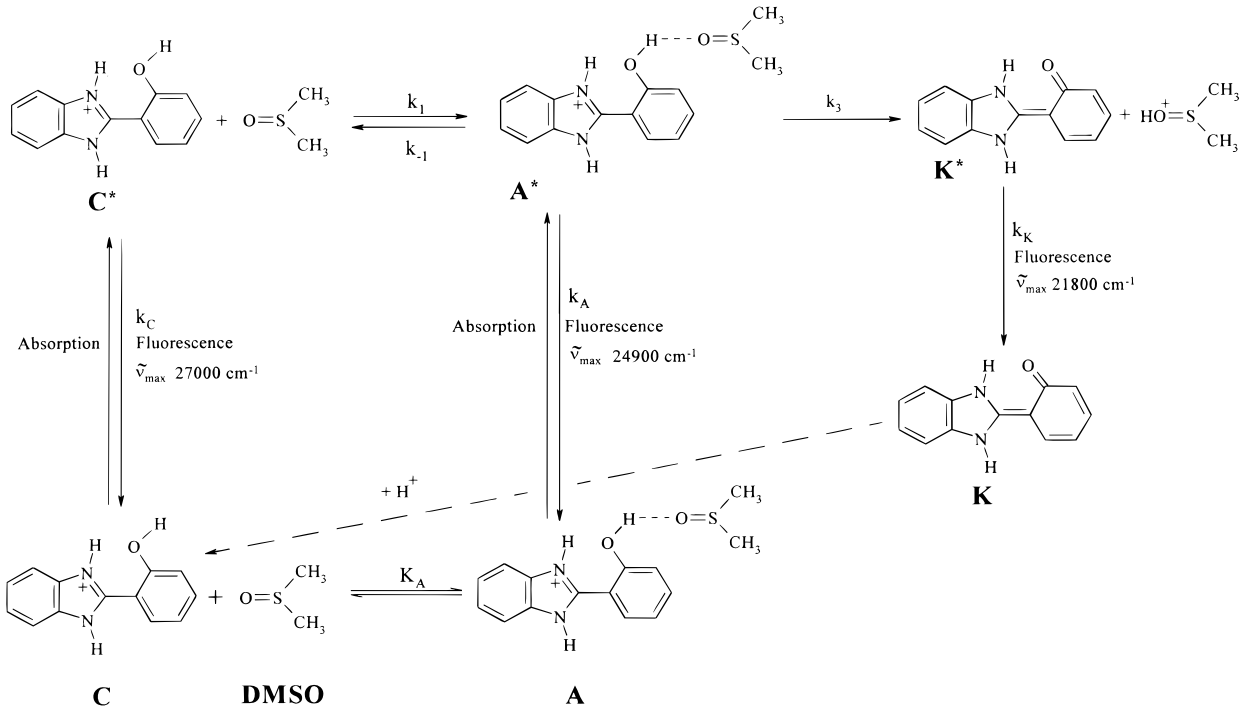

deactivation is assumed to be the formation of **K***,[54,63−65] meaning that this value corresponds essentially to the fluorescence quantum yield of **K***. This hypothesis is supported by the value obtained for the ratio ϕ_K/ϕ_C.

(2) Proton Transfer from C* to Dimethyl Sulfoxide. The absorption spectrum of HBI in acidified acetonitrile in the presence of DMSO (Figure 5) shows changes similar to those observed upon adding MU. Accordingly, the formation of a hydrogen-bonded adduct **A** between **C** and DMSO is proposed (see Scheme 3). The value obtained for the equilibrium constant is $K_A = 13.3 \pm 0.1$ dm^3 mol^{-1}.

The observed changes in the fluorescence emission spectra of HBI upon adding DMSO (quenching of band C and increasing of band K, Figure 1c) indicate that DMSO is able to induce the photodissociation of **C***. This is supported by the fact that for the methoxy derivative MBI no spectral changes were observed when DMSO was added.

From the analysis of the emission spectra of HBI in acidified acetonitrile in the presence of DMSO by the methods of normalization and PCA, we conclude that there exist three independent components in these spectra, whose contributions vary with the concentration of DMSO. The spectra of the components obtained by the two different methods coincide. Figure 10 shows the spectra of these components. Two of the obtained spectral components correspond to the emission of the photoacid **C*** and its conjugate base **K***. The third component resembles the one obtained in the presence of MU (although its emission maximum is slightly shifted to the blue). We can therefore attribute this component to the excited hydrogen-bonded adduct **A*** formed by **C*** and the base DMSO. The experimental spectra at any concentration of DMSO can be perfectly reproduced by linear combinations of the obtained spectral components (Figure 10). Since in this case the maximum of **A*** is close to the maximum of **C***, no shoulder due to **A*** (as detected in the case of MU) is seen in the emission. Instead, a shift of the maximum of band C is observed.

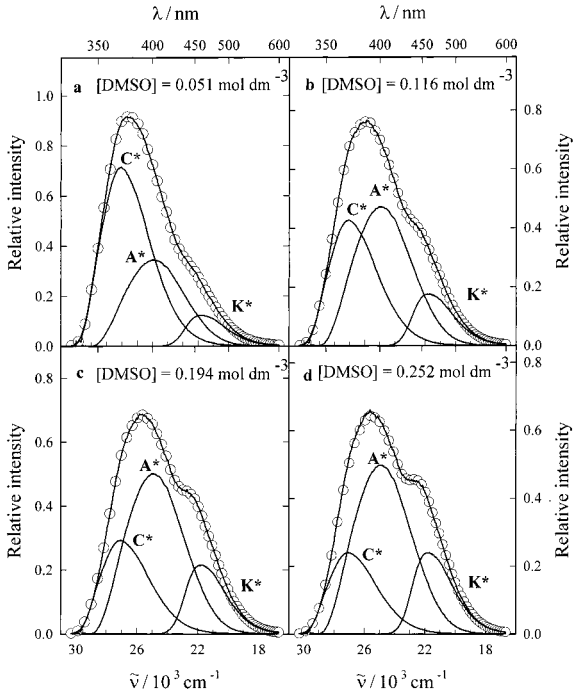

Figure 10. Experimental (—) fluorescence spectra of HBI in acidified acetonitrile solution ([$HClO_4$] = 2.5×10^{-3} mol dm^{-3}) with various dimethyl sulfoxide concentrations and calculated spectra (— ○ —) obtained by fitting a linear combination of the fluorescence spectra of **C***, **A***, and **K***. The individual contributions of these spectra are also shown. $\tilde{\nu}_{exc} = 31\,700$ cm^{-1}. [HBI] = 8.9×10^{-6} mol dm^{-3}.

In Figure 11, the ratios of the emission coefficients of the fluorescent species are plotted against the concentration of DMSO. As can be seen, the ratio between the emission coefficients of the cation (F_C^0/F_C) does not depend linearly on the concentration of DMSO, which is due to the formation of the adduct in the ground state. Furthermore, we observe that the ratio of the emission coefficients of **K*** and **A*** is almost

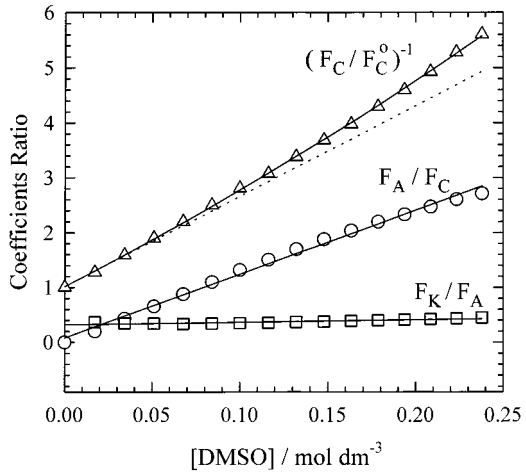

Figure 11. Ratio of the emission coefficients expressing the relative contributions of the individual fluorescence spectra of **C***, **A***, and **K*** to the fluorescence spectra of HBI in acidified acetonitrile solution ($[HClO_4] = 2.5 \times 10^{-3}$ mol dm^{-3}) with increasing dimethyl sulfoxide concentration. F_C^0 is the emission coefficient of **C*** in the absence of DMSO. The broken line illustrates a linear correlation. $\tilde{\nu}_{exc} = 31\,700$ cm^{-1}. [HBI] $= 8.9 \times 10^{-6}$ mol dm^{-3}.

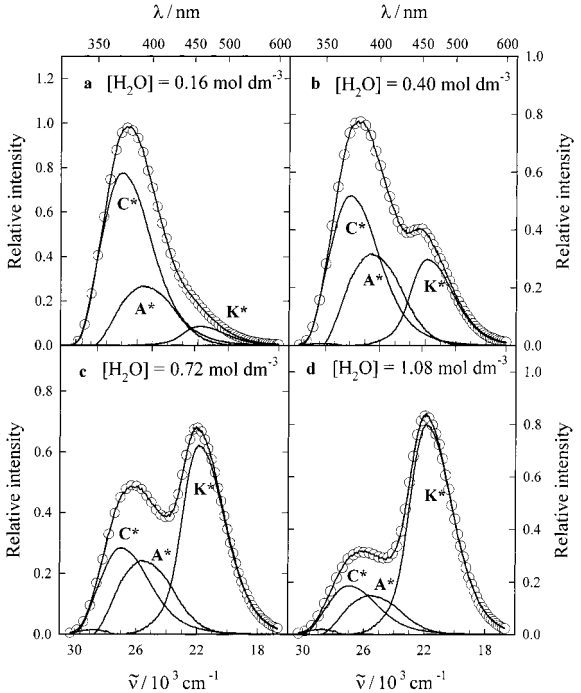

Figure 12. Experimental (—) fluorescence spectra of HBI in acidified acetonitrile solution ($[HClO_4] = 6.0 \times 10^{-4}$ mol dm^{-3}) with various water concentrations and calculated spectra (— ○ —) obtained by fitting a linear combination of the fluorescence spectra of **C***, **A***, and **K***. The individual contributions of these spectra are also shown. $\tilde{\nu}_{exc} = 31\,700$ cm^{-1}. [HBI] $= 8.6 \times 10^{-6}$ mol dm^{-3}.

independent of [DMSO]. This independence was not observed when the base was MU (Figure 9) and reflects that DMSO, unlike MU, does not favor the conversion of **A*** into **K***.

The decay of band C at 27 000 cm^{-1} is biexponential (Figure 6), in contrast to the behavior observed with MU as the base, which gave a monoexponential decay. This biexponential decay is also observed at low concentrations of DMSO, where the contribution of the excited adduct to the emission at 27 000 cm^{-1} is expected to be negligible. This means that in the presence of DMSO the decay of the cation **C*** is biexponential. One of the components shows a decay time which is almost constant and whose contribution to the decay rises when the DMSO concentration is increased, while the decay time and contribution of the other component decreases with increasing DMSO concentration. The reciprocal of this latter decay time does not depend linearly on [DMSO], indicating that the quenching of the cation by DMSO is not a simple process. Probably the formation of the adduct in the excited state is a reversible process.

In agreement with our interpretations above, we propose the mechanism shown in Scheme 3 for the photodissociation of **C*** in the presence of DMSO. The differences between the behavior of the bases DMSO and MU are 2-fold: the formation in the excited state of the adduct between **C*** and the base is reversible in the case of DMSO, and, unlike MU, DMSO does not catalyze the transformation of **A*** into **K***. The equations representing the dependence of the emission coefficients and decay times on the concentration of DMSO allow us to reproduce the experimental behavior very well (see the solid lines in Figure 6), yielding, by means of global analysis, the values of the constants listed in Table 1.[80]

(3) Proton Transfer from C* to Water. Whereas the absorption and fluorescence excitation spectra of HBI in acidified acetonitrile changed in the presence of MU and DMSO, no alteration was observed in the presence of water (Figure 1). Therefore, there is no sign of the existence of a ground-state hydrogen-bonded adduct of the cation **C** with water.

The emission spectra in the presence of water (Figure 1a) showed again the quenching of band C and the rise of band K upon increasing the water concentration, which indicates that the photodissociation of the cation **C*** takes place. It should be noted that no isoemissive point is observed in the series. The method of PCA yielded the presence of three spectral components, which are displayed in Figure 12. The first component (maximum at 27 000 cm^{-1}) corresponds to the cation **C***. The second component, which emits in the intermediate region (maximum at 25 600 cm^{-1}), is similar to the spectrum which was attributed above to the adduct **A*** of the excited cation with MU or DMSO. We associate therefore this component to an excited adduct between **C*** and one molecule of water, which we also call **A*** (see Scheme 4). The third component has a spectrum which is very similar to that of the keto species **K*** in acetonitrile, but not completely identical (it is slightly broader and tails more at high wavenumbers). This spectrum resembles more the spectrum of **K*** in water.[54] This points to a specific solvation effect of **K*** by water as the possible cause of this fact. Each experimental spectrum is satisfactorily reproduced by a linear combination of the spectra of **C***, **A***, and **K*** (Figure 12). Figure 13 shows the values obtained for the relative emission coefficients F of each species at different water concentrations.

The decrease of the emission coefficient of the cation **C*** as the concentration of water increases does not follow the Stern−Volmer relation. This might be due to the reversibility of the quenching process. This hypothesis is supported by the fact that the emission band C decays biexponentially (Figure 2).

The ratio of the emission coefficients of **K*** and **A*** (F_K/F_A) shows a nearly linear dependence on [H_2O] with an intercept equal to zero (see insert in Figure 13), indicating that **K*** can only be formed from **A*** with one molecule of water. Since **A*** is the excited adduct formed between **C*** and one molecule of water, this means that the photodissociation of the cation **C*** requires two molecules in order to take place.

In Scheme 4 our proposed mechanism for the proton transfer from **C*** to water is displayed. As with DMSO, the complexation

SCHEME 4: Mechanism of the Proton Transfer from the Cationic Photoacid C* to the Base Water in Acetonitrile Solution

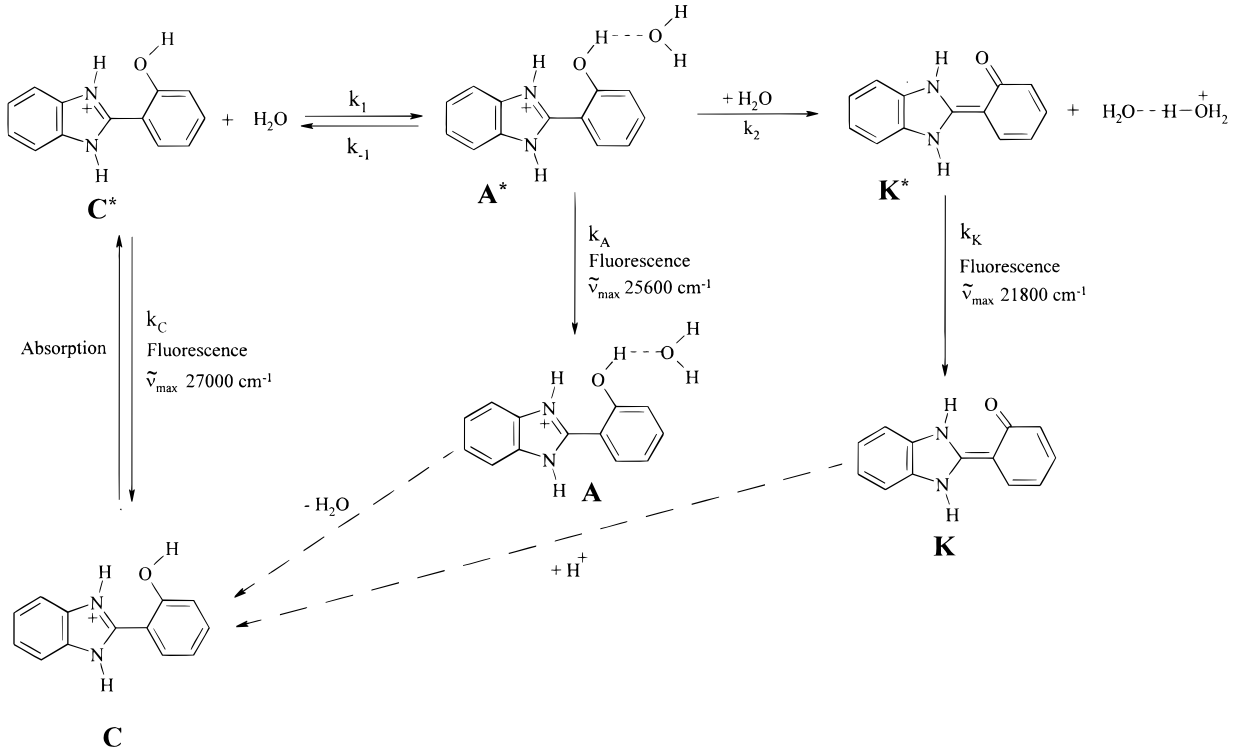

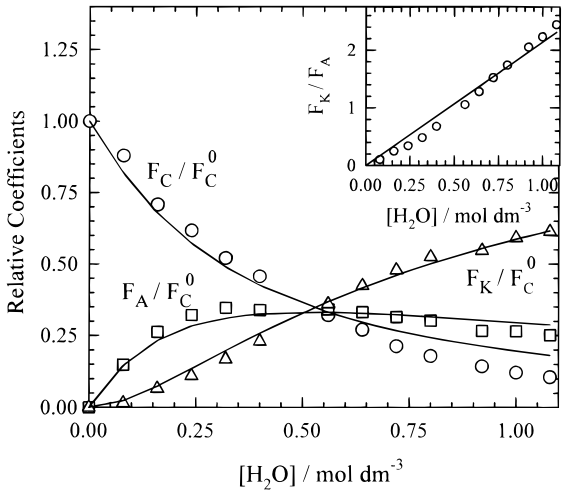

Figure 13. Emission coefficients expressing the relative contributions of the individual fluorescence spectra of **C***, **A***, and **K*** to the fluorescence spectra of HBI in acidified acetonitrile solution ([$HClO_4$] = 6.0×10^{-4} mol dm^{-3}) with increasing water concentration. F_C^0 is the emission coefficient of **C*** in the absence of water. The solid lines are the result of the global fit of the equations deduced from the proposed mechanism in Scheme 4 to represent the dependence of the fluorescence intensities and decay times on water concentration. The insert shows the [H_2O] dependence of the ratio of the emission coefficients of **K*** and **A***. $\tilde{\nu}_{exc}$ = 31 700 cm^{-1}. [HBI] = 8.6×10^{-6} mol dm^{-3}.

in the excited state is reversible, but, in contrast to the behavior observed with the bases DMSO and MU, the direct dissociation process of the adduct to yield **K*** does not occur. A single molecule of water, unlike DMSO and MU, is unable to accept the proton. From this mechanism, the equations representing the dependence of the emission coefficients and decay times on the concentration of water can be deduced.[80] These equations can be fitted satisfactorily to the experimental data (see the solid lines in Figures 3 and 13). Note that the longer decay time of the biexponential decay of band C shows an experimental behavior in agreement with the model, which predicts a slight increase of this decay time at low concentrations, followed by a decrease at higher concentrations (Figure 3). The values of the rate constants obtained by means of a global fit of all the equations are listed in Table 1. It can be observed in Figures 3 and 13 that the goodness of the fit to the data corresponding to the short decay times is somewhat inferior. It should be taken into account, however, that the short decay times (around 0.4 ns) are close to the resolution limit of our equipment (0.1 ns) and therefore have a larger uncertainty than the long decay times.

(4) Comparative Discussion. The lifetime and fluorescence spectrum of the excited adduct **A*** formed between the photoacid **C*** and one molecule of the base (MU, DMSO, or water) are similar for the three investigated bases. The adduct has its emission maximum between that of **C*** and **K***. This indicates that the hydrogen bond between the OH group and the base should be quite strong, giving the adduct some photophysical properties between those of the photoacid **C***, without the transfer of the proton, and its conjugate base **K***, with the proton transferred.

The quantum yields of the three adducts (Table 1) are very similar and of the same order of magnitude as the quantum yield of the cation **C***. The ratio of quantum yields ϕ_K/ϕ_C, which is independent of the nature of the base, should have the same value in the three cases. As can be seen in Table 1, the found values are indeed the same within the experimental error.

The values obtained for the rate constant k_1 (formation of the adduct in the excited state) are between 3.5 and 5×10^9 dm^3 mol^{-1} s^{-1} (Table 1). These values can be considered to correspond to a diffusion-controlled process, since a steric factor must exist that takes into account the orientation of the reactants to form the adduct.

The rate constant k_{-1} (dissociation of the adduct to regenerate the reactants) changes significantly with the nature of the base, the highest value being obtained for water (Table 1). In the case

of MU this constant could not be determined, because it is much lower than the values for the rate constants of the other deactivation routes of the adduct. This means that its value cannot be higher than $\sim 1 \times 10^7$ s^{-1} (10% of the rate constant of the slowest deactivation route of **A***); otherwise it would have been observed experimentally.

Knowing the values of the rate constants k_1 and k_{-1}, we can calculate the equilibrium constants of formation of the adducts in the excited state, $K_{A*} = k_1/k_{-1}$, yielding the values given in Table 1. A decrease of the equilibrium constant is observed in the following order: K_{A*}(MU) > K_{A*}(DMSO) > K_{A*}(water). This order changes for the values obtained for the ground-state equilibria, K_A(DMSO) $\cong$ K_A(MU) > K_A(water), but in both cases water is the species with the lowest tendency to complexate, its adduct probably being the least stable. These results are in agreement with the hydrogen-bond acceptor basicities of Kamlet−Taft for these species, since the value for water (0.18) is much lower than the value for DMSO (0.76) and for species similar to MU, like dimethylformamide (0.69) or formamide (0.55).[81] For the same base, the association constants are higher in the excited state than in the ground state, which is in agreement with the higher acidity of **C*** in the excited state. Similar results were obtained for other excited adducts of hydroxyaromatic compounds, which show an increase of the formation equilibrium constants by 1−2 orders of magnitude on photoexcitation.[13] On studying the solvatochromic shifts of the photoacids β-naphthol and 5-cyano-2-naphthol, Solntsev et al. found also an excited-state strengthening of the hydrogen bond to the solvent.[72−74]

The stronger hydrogen bond of the adducts in the excited state than in the ground state is demonstrated also by the red shift of the absorption and fluorescence spectra upon formation of the adducts.[68] The position of the emission maximum of the adducts changes with the base, showing a red shift in the order water (25 600 cm^{-1}), DMSO (24 900 cm^{-1}), and MU (23 900 cm^{-1}). This points to a strengthening of the hydrogen bond of the excited adducts in the same order, in agreement with the obtained values of the equilibrium constants K_{A*} (Table 1).

The proton transfer takes place by dissociation of the adduct via two different processes, one of them unimolecular and the other bimolecular with a second molecule of the base. In the bimolecular dissociation process, finally a cluster of two molecules of the base is the accepting entity of the proton. The rate constant k_2 of the bimolecular dissociation of the adduct is lower than that of a diffusion-controlled process (Table 1), indicating that the process is chemically controlled. The highest value is found for MU, probably due to the fact that its basicity is significantly higher than that of the other two bases. This process has not been observed for DMSO, possibly because of the low concentration of DMSO used (maximum concentration 0.25 mol dm^{-3}, whereas 1.08 mol dm^{-3} for water) and because of the lower value of k_2 for this species.

The unimolecular dissociation of the adduct yielding **K*** and the protonated base (with rate constant k_3) has been detected for the bases DMSO and MU, but not for water. Apparently one molecule of water is unable to accept the proton in a process fast enough to compete with the other processes undergone by the adduct. In the case of water, a cluster of two molecules is therefore the entity that finally accepts the proton donated by the photoacid.

Conclusion

We investigated the mechanism of the photoinduced proton transfer from the excited protonated cation of 2-(2′-hydroxyphenyl)benzimidazole **C***. The proton transfer from **C*** to the three investigated bases (water, dimethyl sulfoxide, and methylurea) in acetonitrile solution occurs exclusively via a 1:1 hydrogen-bonded adduct **A*** between **C*** and the base. The adduct is formed in the excited state with a diffusion-controlled rate constant. For the bases MU and DMSO, the adduct also exists in the ground state and can reach the excited state by the absorption of light. The fluorescence spectrum and quantum yield of the adducts have been determined as well as some of the equilibrium constants of formation of the adducts in the ground and excited states.

The proton transfer from the photoacid **C*** to the base takes place during the dissociation of the adduct. The unimolecular dissociation, which yields **K*** and the protonated base, has been observed for the adducts formed with MU and DMSO, but was not detected for the adduct formed with water. This led us to the conclusion that one molecule of water is unable to accept the proton from the photoacid; at least this process is not fast enough to compete with the other processes undergone by the adduct. The dissociation of the adduct formed with water requires the assistance of a second molecule of water, and, as a result, the entity which finally accepts the proton is a cluster of two molecules of water. This bimolecular dissociation process of the adduct, whose rate constant is lower than the diffusion-controlled limit, also exists when the base is MU, but was not observed for DMSO.

Acknowledgment. The authors are grateful to J. Luis Pérez-Lustres for assistance and helpful discussion. Support from the spanish Ministerio de Educación y Cultura (Dirección General de Enseñanza Superior, Project PB97-0547) and the Xunta de Galicia (Infraestructura program) is gratefully acknowledged. J.C.P. thanks the Xunta de Galicia for a postgraduate research grant.

Supporting Information Available: Text describing the principal steps of the deduction of eqs 2−4 and tables listing the fluorescence decay times, amplitudes, and χ^2 values determined for HBI at various emission wavenumbers and concentrations of water, MU, and DMSO. This material is available free of charge via the Internet at http://pubs.acs.org.

References and Notes

(1) (a) Eigen, M. *Angew. Chem., Int. Ed. Engl*. **1964**, *3*, 1. (b) Eigen, M.; Kruse, W.; Maass, G.; De Maeyer, L. *Prog. React. Kinet*. **1964**, *2*, 285.

(2) Bell, R. P. *The Proton in Chemistry*, 2nd ed.; Chapman and Hall: London, 1973.

(3) *Proton-Transfer Reactions*; Caldin, E. F., Gold, V., Eds.; Chapman and Hall: London, 1975.

(4) *Electron and Proton Transfer in Chemistry and Biology*; Müller, A., Ratajczak, H., Junge, W., Diemann, E., Eds.; Elsevier: Amsterdam, 1992.

(5) Simmons, E. L. *Prog. React. Kinet.* **1977**, *8*, 161.

(6) (a) Hibbert, F. *Acc. Chem. Res*. **1984**, *17*, 115. (b) Hibbert, F. *Adv. Phys. Org. Chem*. **1986**, *22*, 113.

(7) *Spectroscopy and Dynamics of Elementary Proton Transfer in Polyatomic Systems*; Barbara, P. F., Trommsdorff, H. P., Eds.; Special issue of *Chemical Physics* **1989**, *136*, 153−360.

(8) Ando, K.; Hynes, J. T. In *Structure and Reactivity in Aqueous Solution*; Cramer, C. J., Truhlar, D. G., Eds.; American Chemical Society: Washington, DC, 1994; pp 143−153.

(9) Borgis, D. In *Electron and Proton Transfer in Chemistry and Biology*; Müller, A., Ratajczak, H., Junge, W., Diemann, E., Eds.; Elsevier: Amsterdam, 1992; pp 345−362.

(10) Alhambra, C.; Gao, J.; Corchado, J. C.; Villà, J.; Truhlar, D. G. *J. Am. Chem. Soc*. **1999**, *121*, 2253.

(11) Weller, A. *Prog. React. Kinet*. **1961**, *1*, 188.

(12) Ireland, J. F.; Wyatt, P. A. H. *Adv. Phys. Org. Chem*. **1976**, *12*, 131.

(13) Martynov, I. Yu.; Demyashkevich, A. B.; Uzhinov, B. M.; Kuz'min, M. G. *Russ. Chem. Rev. (Usp. Khim.)* **1977**, *46*, 1.
(14) Rentzepis, P. M.; Barbara, P. F. *Adv. Chem. Phys*. **1981**, *47* (2), 627.
(15) Huppert, D.; Gutman, M.; Kaufmann, K. J. *Adv. Chem. Phys*. **1981**, *47* (2), 643.
(16) Arnaut, L. G.; Formosinho, S. J. *J. Photochem. Photobiol. A: Chem*. **1993**, *75*, 1.
(17) Tolbert, L. M.; Haubrich, J. E. *J. Am. Chem. Soc*. **1994**, *116*, 10593.
(18) Wan, P.; Shukla, D. *Chem. Rev*. **1993**, *93*, 571.
(19) Kalyanasundaram, K. In *Photochemistry in Organized and Constrained Media*; Ramamurthy, V., Ed.; VCH: New York, 1991; pp 39−77.
(20) Linares-Samaniego, S.; Tolbert, L. M. *J. Am. Chem. Soc*. **1996**, *118*, 9974.
(21) Mansueto, E. S.; Wight, C. A. *J. Am. Chem. Soc*. **1989**, *111*, 1900.
(22) Lee, J.; Griffin, R. D.; Robinson, G. W. *J. Chem. Phys*. **1985**, *82*, 4920.
(23) Robinson, G. W.; Thistlethwaite, P. J.; Lee, J. *J. Phys. Chem*. **1986**, *90*, 4224.
(24) Lee, J.; Robinson, G. W.; Web, S. P.; Philips, L. A.; Clark, J. H. *J. Am. Chem. Soc*. **1986**, *108*, 6538.
(25) Lee, J.; Robinson, G. W.; Bassez, M.-P. *J. Am. Chem. Soc*. **1986**, *108*, 7477.
(26) Lee, J. *J. Am. Chem. Soc*. **1989**, *111*, 427.
(27) Krishnan, R.; Lee, J.; Robinson, G. W. *J. Phys. Chem*. **1990**, *94*, 6365.
(28) Fillingim, T. G.; Luo, N.; Lee, J.; Robinson, G. W. *J. Phys. Chem*. **1990**, *94*, 6368.
(29) Krishnan, R.; Fillingim, T. G.; Lee, J.; Robinson, G. W. *J. Am. Chem. Soc*. **1990**, *112*, 1353.
(30) Robinson, G. W. *J. Phys. Chem*. **1991**, *95*, 10386.
(31) Pines, E.; Huppert, D. *Chem. Phys. Lett*. **1986**, *88*, 126.
(32) Pines, E.; Huppert, D. *J. Chem. Phys*. **1986**, *84*, 3576.
(33) Pines, E.; Huppert, D.; Agmon, N. *J. Chem. Phys*. **1988**, *88*, 5620.
(34) Agmon, N.; Pines, E.; Huppert, D. *J. Chem. Phys*. **1988**, *88*, 5631.
(35) Agmon, N. *J. Chem. Phys*. **1988**, *88*, 5639.
(36) Agmon, N. *J. Chem. Phys*. **1988**, *89*, 1524.
(37) Pines, E.; Huppert, D. *J. Am. Chem. Soc*. **1989**, *111*, 4096.
(38) Pines, E.; Huppert, D.; Agmon, N. *J. Phys. Chem*. **1991**, *95*, 666.
(39) Agmon, N.; Huppert, D.; Masad, A.; Pines, E. *J. Phys. Chem*. **1991**, *95*, 10407; **1992**, *96*, 2020.
(40) Goldberg, S. Y.; Pines, E.; Huppert, D. *Chem. Phys. Lett*. **1992**, *192*, 77.
(41) Agmon, N.; Goldberg, S. Y.; Huppert, D. *J. Mol. Liq*. **1995**, *64*, 161.
(42) Pines, E.; Tepper, D.; Magnes, B.-Z.; Pines, D.; Barak, T. *Ber. Bunsen-Ges. Phys. Chem*. **1998**, *102*, 504.
(43) Tolbert, L. M.; Haubrich, J. E. *J. Am. Chem. Soc*. **1990**, *112*, 8163.
(44) Tolbert, L. M.; Harvey, L. C.; Lum, R. C. *J. Phys. Chem*. **1993**, *97*, 13335.
(45) Carmeli, I.; Huppert, D.; Tolbert, L. M.; Haubrich, J. E. *Chem. Phys. Lett*. **1996**, *260*, 109.
(46) Than Htun, M.; Suwaiyan, A.; Klein, U. K. A. *Chem. Phys. Lett*. **1995**, *243*, 71.
(47) Than Htun, M.; Suwaiyan, A.; Klein, U. K. A. *Chem. Phys. Lett*. **1995**, *243*, 506.
(48) Than Htun, M.; Suwaiyan, A.; Klein, U. K. A. *Chem. Phys. Lett*. **1995**, *243*, 512.
(49) Pines, E.; Pines, D.; Barak, T.; Magnes, B. Z.; Tolbert, L. M.; Haubrich, J. E. *Ber. Bunsen-Ges. Phys. Chem*. **1998**, *102*, 511.
(50) Gopich, I. V.; Solntsev, K. M.; Agmon, N. *J. Chem. Phys*. **1999**, *110*, 2164.
(51) Agmon, N. *J. Chem. Phys*. **1999**, *110*, 2175.
(52) Pines, E.; Fleming, G: R. *J. Phys. Chem*. **1991**, *95*, 10448.
(53) Davila, J.; Bignozzi, C. A.; Scandola, F. *J. Phys. Chem*. **1989**, *93*, 1373.
(54) Mosquera, M.; Penedo, J. C.; Ríos Rodríguez, M. C.; Rodríguez-Prieto, F. *J. Phys. Chem*. **1996**, *100*, 5398.
(55) Mosquera, M.; Ríos Rodríguez, M. C.; Rodríguez-Prieto, F. *J. Phys. Chem. A* **1997**, *101*, 2766.
(56) Pina, F.; Melo, M. J.; Santos, H.; Lima, J. C.; Abreu, I.; Ballardini, R.; Maestri, M. *New. J. Chem*. **1998**, *22*, 1093.
(57) Pina, F.; Melo, M. J.; Parola, A. J.; Maestri, M.; Balzani, V. *Chem. Eur. J*. **1998**, *4*, 2001.
(58) Bardez, E.; Chatelain, A.; Larrey, B.; Valeur, B. *J. Phys. Chem*. **1994**, *98*, 2357.
(59) Bardez, E.; Fedorov, A.; Berberan-Santos, M. N.; Martinho, J. M. G. *J. Phys. Chem. A* **1999**, *103*, 4131.
(60) Bardez, E. *Isr. J. Chem*. **1999**, *39*, 319.
(61) Perdoncin, G.; Scorrano, G. *J. Am. Chem. Soc*. **1977**, *99*, 6983.
(62) Hall, N. F. *J. Am. Chem. Soc*. **1930**, *52*, 5115.
(63) Douhal, A.; Amat-Guerri, F.; Lillo, M. P.; Acuña, A. U. *J. Photochem. Photobiol. A: Chem*. **1994**, *78*, 127.
(64) Das, K.; Sarkar, N.; Majumdar, D.; Bhattacharyya, K. *Chem. Phys. Lett*. **1992**, *198*, 443.
(65) Das, K.; Sarkar, N.; Ghosh, A. K.; Majumdar, D. Nath, D. N.; Bhattacharyya, K. *J. Phys. Chem*. **1994**, *98*, 9126.
(66) Homer, R. B.; Johnson, C. D. In *The Chemistry of Amides*; Zabicky, J., Ed.; Interscience: London, 1970; p 187.
(67) Beens, H.; Grellmann, K. H.; Gurr, M.; Weller, A. H. *Discuss. Faraday Soc*. **1965**, *39*, 183.
(68) Mataga, N.; Kubota, T. *Molecular Interactions and Electronic Spectra*; Dekker: New York, 1970.
(69) Hasselbacher, C. A.; Waxman, E.; Galati, L. T.; Contino, P. B.; Ross, J. B. A.; Laws, W. R. *J. Phys. Chem*. **1991**, *95*, 2995.
(70) Timoneda, J. J.; Hynes, J. T. *J. Phys. Chem*. **1991**, *95*, 10431.
(71) Bisht, P. B.; Joshi, G. C.; Tripathi, H. B. *Chem. Phys. Lett*. **1995**, *237*, 356.
(72) Solntsev, K. M.; Huppert, D.; Tolbert, L. M.; Agmon, N. *J. Am. Chem. Soc*. **1998**, *120*, 7981.
(73) Solntsev, K. M.; Huppert, D.; Agmon, N. *J. Phys. Chem. A* **1998**, *102*, 9599.
(74) Solntsev, K. M.; Huppert, D.; Agmon, N. *J. Phys. Chem. A* **1999**, *103*, 6984.
(75) Lawton, W. H.; Sylvestre, E. A. *Technometrics* **1971**, *13*, 617.
(76) Wold, S. *Technometrics* **1978**, *20*, 397.
(77) Mazzucato, U.; Monicchioli, F. *Chem. Rev*. **1991**, *91*, 1679.
(78) Saltiel, J.; Choi, J.-O.; Sears, D. F., Jr.; Eaker, D. W.; O'Shea, K. E.; García, I. *J. Am. Chem. Soc*. **1996**, *118*, 7478.
(79) Saltiel, J.; Zhang, Y.; Sears, D. F., Jr. *J. Phys. Chem. A* **1997**, *101*, 7053.
(80) Penedo, J. C. Photoinduced Inter- and Intramolecular Proton Transfer in Benzimidazole Derivatives. Influence of Tautomerism and Conformational Isomerism. Ph.D. Thesis, University of Santiago de Compostela, Spain, 1998.
(81) Reichardt, C. *Solvents and Solvent Effects in Organic Chemistry*, 2nd ed.; VCH: Weinheim, Germany, 1988.